PERGAMON

International Journal of Plasticity 18 (2002) 345–358

INTERNATIONAL JOURNAL OF Plasticity

www.elsevier.com/locate/ijplas

# Steady crack growth in elastic–plastic fluid-saturated porous media

Enrico Radi [a,*], Davide Bigoni [b], Benjamin Loret [c]

[a]Dipartimento di Ingegneria Strutturale, Università di Cagliari, Piazza d'Armi 19- 09123 Cagliari, Italy
[b]Dipartimento di Ingegneria Meccanica e Strutturale, Università di Trento, Via Mesiano 77, 38050 Povo, Trento, Italy
[c]Institut de Mécanique de Grenoble, Laboratoire Sols Solides Structures, BP 53X- 38041 Grenoble, France

Received in final revised form 28 September 1999

**Abstract**

An asymptotic solution is obtained for stress and pore pressure fields near the tip of a crack steadily propagating in an elastic–plastic fluid-saturated porous material displaying linear isotropic hardening. Quasi-static crack growth is considered under plane strain and Mode I loading conditions. In particular, the effective stress is assumed to obey the Drucker–Prager yield condition with associative or non-associative flow-rule and linear isotropic hardening is adopted. Both permeable and impermeable crack faces are considered. As for the problem of crack propagation in poroelastic media, the behavior is asymptotically drained at the crack-tip. Plastic dilatancy is observed to have a strong effect on the distribution and intensity of pore water pressure and to increase its flux towards the crack-tip. 

*Keywords:* A. Crack propagation; Fluid-saturated elastic–plastic materials; C. Asymptotic analysis

## 1. Introduction

Parts of earth's shallow crust infiltrated with ground water or oil have a mechanical response complicated by elastic–plastic deformation coupled with diffusion of pore fluid. Hydraulic fracturing is often used in these media to enhance gas or oil production. In addition to the interest in this technique, time-dependent geophysical phenomena such as propagation of aseismic slips and following deformations have focussed

* Corresponding author. Tel.: +39-70-675-5431; fax: +39-70-675-5418.
*E-mail address:* radi@vaxca1.unica.it (E. Radi).


PII: S0749-6419(00)00101-7

research on fracture mechanics in viscous or inviscid poroelastic materials (Rice and Cleary, 1976; Rice and Simons, 1976; Cleary, 1978; Rudnicki, 1985; 1991; Atkinson and Craster, 1991; Rudnicki and Koutsibelas, 1991; Desroches et al., 1994). However, neglecting plastic behavior of the solid skeleton represents only a first approximation. For instance, Johnson and Cleary (1991), van den Hoek et al. (1993) and Papanastasiou (1997) suggest that linear elastic crack propagation models may underestimate the down-hole pressure measured during field operations for hydraulic fracturing. As a matter of fact, it will be shown in this paper — with reference to steady crack propagation — that plastic dilatancy strongly affects the pore pressure distribution at the crack-tip. There are few contributions that account for the elastic-plastic behavior of fluid-saturated porous media when analyzing crack propagation. Plastic dilatancy effects at the crack-tip were analyzed by van den Hoek et al. (1993) and Mohr-Coulomb elastoplasticity was considered during crack propagation by Papanastasiou and Thiercelin (1993) and Papanastasiou (1997), using a combined finite difference/finite element technique.

In this article, an asymptotic solution is obtained for steady-state crack propagation under plane strain, mode I conditions. Propagation occurs in a porous, fluid-saturated material characterized by an elastoplastic skeleton obeying a Drucker–Prager yield criterion with volumetric non-associative flow law and isotropic hardening. The technique used to solved this asymptotic problem was initiated by Amazigo and Hutchinson (1977) and developed in various directions, but always for a single phase solid, by Achenbach et al. (1981), Zhang et al. (1983), Ponte Castañeda (1987), Östlund and Gudmundson (1988), Bose and Ponte Castañeda (1992), Bigoni and Radi (1993; 1996), Radi and Bigoni (1993; 1994; 1996), Herrmann and Potthast (1995). Here, the mechanical behavior of the elastic-plastic medium is described through coupled constitutive equations developed, in the framework of the theory of mixtures, by Loret and Harireche (1991), where the Darcy's law is used to model the fluid diffusion process. Since the ductility of these materials is small compared with metals, as shown by the experimental data reported by Khan et al. (1991, 1992) for Berea sandstone, it is reasonable to consider the small deformation incremental theory. Moreover, both problems of permeable and impermeable crack faces are considered.

Like for poroelasticity, the behavior is asymptotically drained at the crack-tip. The results demonstrate that the explicit coupling between plastic dilatancy and fluid compressibility yields a peculiar behavior of the pore pressure near the crack-tip. Dilatancy increases the flux of water towards the crack-tip, but also the water pressure since in this asymptotic analysis the latter is not controlled at finite distance from the crack-tip. Moreover, the flux of fluid together with plasticity effects may dissipate the amount of supplied energy, leading to a reduction of the energy available to fracture the material.

## 2. Constitutive equations

We refer to the elastic–plastic model for fluid-saturated porous media proposed by Loret and Harireche (1991), that is summarized here. Within the context of small deformation incremental theory, both the strain rate $\dot{\boldsymbol{\varepsilon}}$ of the solid skeleton and the rate of fluid mass content per unit reference volume $\dot{\zeta}$ are decomposed into an elastic part and a plastic part, denoted by the respective indices $(\ )^e$ and $(\ )^p$, namely

$$\dot{\boldsymbol{\varepsilon}} = \dot{\boldsymbol{\varepsilon}}^e + \dot{\boldsymbol{\varepsilon}}^p, \quad \dot{\zeta} = \dot{\zeta}^e + \dot{\zeta}^p. \tag{1}$$

The elastic strain rates $\dot{\boldsymbol{\varepsilon}}^e$ and $\dot{\zeta}^e$ are related to the rates of total stress $\dot{\boldsymbol{\sigma}}$ and pore pressure $\dot{p}$ through isotropic constitutive equations that involve four material coefficients, namely, Biot (1941; 1956), Rice and Cleary (1976), the drained Young's modulus $E>0$ and Poisson's ratio $\nu \in [-1, \ 1/2]$, the undrained Poisson's ratio $\nu_u \in [\nu, 1/2]$, and the Skempton coefficient $B>0$. The above restrictions on the material coefficients ensure positive definiteness of the elastic constitutive equations in terms of the strain and stress pairs, $(\boldsymbol{\varepsilon}, \zeta)$ and $(\boldsymbol{\sigma}, p)$ respectively. In explicit form,

$$\dot{\boldsymbol{\varepsilon}}^e = \frac{1-2\nu}{E}\left(\frac{1}{3}\ \mathrm{tr}\dot{\boldsymbol{\sigma}} + \alpha\ \dot{p}\right)\mathbf{I} + \frac{1+\nu}{E}\ \mathrm{dev}\dot{\boldsymbol{\sigma}}, \tag{2}$$

$$\dot{\zeta}^e = \frac{1-2\nu}{E}\alpha\left(\mathrm{tr}\dot{\boldsymbol{\sigma}} + \frac{3}{B}\ \dot{p}\right), \tag{3}$$

where $\mathbf{I}$ is the second order identity tensor and dev $\dot{\boldsymbol{\sigma}}$ denotes the deviatoric part of $\dot{\boldsymbol{\sigma}}$. The coefficient $\alpha$ enters the effective stress (compressive pore pressure is positive)

$$\boldsymbol{\sigma}^* = \boldsymbol{\sigma} + \alpha p \mathbf{I}, \tag{4}$$

which is related directly to the elastic strain $\boldsymbol{\varepsilon}^e$ through the drained coefficients $E$ and $\nu$. During undrained loading in the elastic regime, $\dot{\zeta}^e = 0$ and the strain rate is related to the total stress rate $\dot{\boldsymbol{\sigma}}$ through the undrained coefficients $E_u$ and $\nu_u$, namely

$$\dot{\boldsymbol{\varepsilon}}^e = \frac{1-2\nu_u}{3\ E_u}(\mathrm{tr}\dot{\boldsymbol{\sigma}})\ \mathbf{I} + \frac{1+\nu_u}{E_u}\ \mathrm{dev}\dot{\boldsymbol{\sigma}}, \quad \dot{p} = -\frac{B}{3}\mathrm{tr}\dot{\boldsymbol{\sigma}}. \tag{5}$$

Since water can not sustain shear stresses, the drained and undrained shear compliances must be identical, i.e. $(1+\nu)/E = (1+\nu_u)/E_u$, and then the Biot coefficient $\alpha$ can be expressed in terms of $B$, $\nu$ and $\nu_u$, namely:

$$\alpha = \frac{3}{B}\frac{\nu_u - \nu}{(1-2\nu)(1+\nu_u)}. \tag{6}$$

To close the system of differential equations, we assume that diffusion of pore fluid obeys Darcy's law and we require the fluid mass continuity,

$$\mathbf{q} = -\rho_0\ \kappa\ \nabla p, \quad \rho_0\ \dot{\zeta} = -\mathrm{div}\ \mathbf{q}, \tag{7}$$

where $\mathbf{q}$ is the mass flux, $\kappa$ is the permeability coefficient (unit: time × length$^3$/ mass), $\rho_0$ is the reference density, and $\nabla$ and div are the gradient and divergence operators respectively.

The yield condition is expressed in terms of the effective stress $\boldsymbol{\sigma}^*$. It is of the Drucker–Prager type and it incorporates pressure-sensitivity through the coefficient $\mu > 0$, namely

$$f(\boldsymbol{\sigma}^*, k) = \sqrt{J_2(\boldsymbol{\sigma}^*)} + \frac{\mu}{3}\mathrm{tr}\boldsymbol{\sigma}^* - k = 0, \tag{8}$$

where

$$J_2(\boldsymbol{\sigma}^*) = \frac{1}{2}|\mathrm{dev}\boldsymbol{\sigma}^*|^2 = \frac{1}{2}|\mathrm{dev}\boldsymbol{\sigma}|^2, \tag{9}$$

is the second invariant of the deviatoric effective stress, $k$ is an internal variable governing the isotropic hardening behavior. The fact that the stress enters the set of state variables through the Biot effective stress $\boldsymbol{\sigma}^*$ rather than through the more usual Terzaghi effective stress $\boldsymbol{\sigma} + p\,\mathbf{I}$, as usually assumed, e.g. Rudnicki (1984), simplifies slightly the algebra. Rice (1977) has argued on theoretical grounds that the macroscopic effective stress appropriate to describe inelasticity effects arising from opening of microcracks and sliding on small areas of contact is Terzaghi effective stress. However, as the coefficient $\alpha$ is close to 1 for rocks, usually between 0.5 and 1, and very close to 1 for soils, the difference on the plastic behaviour between the two formulations is hard to quantify. To our knowledge, no discriminant argument of *quantitative* nature has been presented so far in favor of one formulation over the other.

Let $\mathbf{Q}$ and $\varphi$ denote the derivative of the yield function (8) with respect to the effective stress tensor $\boldsymbol{\sigma}^*$ and to the pore pressure $p$, respectively:

$$\mathbf{Q} = \frac{\partial f}{\partial \boldsymbol{\sigma}^*} = \frac{\mathrm{dev}\boldsymbol{\sigma}}{2\sqrt{J_2(\boldsymbol{\sigma})}} + \frac{\mu}{3}\,\mathbf{I}, \quad \varphi = \frac{\partial f}{\partial p} = \alpha\ \mu, \tag{10}$$

since dev $\boldsymbol{\sigma}^* =$ dev $\boldsymbol{\sigma}$, as it follows from (4).

The evolution law for the plastic internal variable allows for non-associative flow-rule and linear isotropic hardening behavior, namely:

$$\dot{\boldsymbol{\varepsilon}}^p = \Lambda\ \mathbf{P}, \quad \dot{\zeta}^p = \Lambda\ \phi, \quad \dot{k} = \Lambda\ H, \tag{11}$$

where $\Lambda \geqslant 0$ is the (non negative) plastic multiplier and $H > 0$ the hardening modulus, assumed to be strictly positive and constant for linear isotropic hardening behavior. The plastic flow direction $\mathbf{P}$ has both a deviatoric and a volumetric component introduced by the plastic dilatancy parameter $\beta \in [0,\ \mu]$, namely,

$$\mathbf{P} = \frac{\mathrm{dev}\boldsymbol{\sigma}}{2\sqrt{J_2(\boldsymbol{\sigma})}} + \frac{\beta}{3}\mathbf{I}, \quad \phi = \alpha\ \beta. \tag{12}$$

The consistency condition $\dot{f}(\boldsymbol{\sigma}^*, k) = 0$ together with (10) and $(11)_3$ yields the plastic multiplier $\Lambda$:

$$\Lambda = \frac{1}{H}\langle \mathbf{Q}\cdot\dot{\boldsymbol{\sigma}}^* \rangle = \frac{1}{H}\langle \mathbf{Q}\cdot\dot{\boldsymbol{\sigma}} + \alpha\ \mu\ \dot{p} \rangle, \tag{13}$$

where the symbol $\langle\ \rangle$ denotes the Macaulay operator, namely, for every real value $x$, $\langle x \rangle = \max\{x, 0\}$.

Plastic flow occurs when the stress point lies on the yield surface (8), that is $f(\boldsymbol{\sigma}^*, k) = 0$ and $\mathbf{Q}\cdot\dot{\boldsymbol{\sigma}}^* > 0$, while elastic unloading occurs whenever $f(\boldsymbol{\sigma}^*, k) < 0$ or $\mathbf{Q}\cdot\boldsymbol{\sigma}^* \leqslant 0$. So when the stress point lies on the yield surface (8), the elastic–plastic rate constitutive equations can be written in the form:

$$\dot{\boldsymbol{\varepsilon}} = \frac{1}{E}\left[(1-2\nu)\left(\frac{1}{3}\mathrm{tr}\dot{\boldsymbol{\sigma}} + \alpha\ \dot{p}\right)\mathbf{I} + (1+\nu)\ \mathrm{dev}\dot{\boldsymbol{\sigma}} + \frac{1}{h}\langle \mathbf{Q}\cdot\dot{\boldsymbol{\sigma}} + \alpha\ \mu\ \dot{p} \rangle \mathbf{P}\right], \tag{14}$$

$$\dot{\zeta} = \frac{1}{E}\left[\alpha(1-2\nu)\left(\mathrm{tr}\dot{\boldsymbol{\sigma}} + \frac{3}{B}\dot{p}\right) + \frac{1}{h}\langle \mathbf{Q}\cdot\dot{\boldsymbol{\sigma}} + \alpha\ \mu\ \dot{p} \rangle\ \alpha\ \beta\right], \tag{15}$$

where we have introduced the dimensionless hardening modulus $h = \mathrm{H}/\mathrm{E}$; otherwise, the rate constitutive relationship reduces to the poroelastic equations, obtained by setting $\Lambda = 0$.

Note that, for $\beta = \mu$, the rate constitutive equations become associative in the sense that the elastic-plastic stiffness and compliance expressed in terms of the pairs $(\boldsymbol{\varepsilon}, \zeta)$ and $(\boldsymbol{\sigma}, p)$ are symmetric.

## 3. Crack propagation problem

The problem of a plane crack propagating at constant velocity $c$ along a rectilinear path in an infinite medium is now considered. The mechanical behavior of the material is described by the incremental elastic–plastic constitutive model presented in Section 2. This framework allows for possible sectors of elastic unloading which may develop in the proximity of the crack-tip, during crack propagation. A cylindrical coordinate system $(O, \mathbf{e}_r, \mathbf{e}_\vartheta, \mathbf{e}_3)$ moving with the crack-tip towards the $\vartheta = 0$ direction is considered, with the $x_3$-axis aligned with the straight crack front. The steady-state condition yields the following time derivative rule, for any scalar, vector or second order tensor $\mathbf{A}$:

$$\dot{\mathbf{A}} = c\left(r^{-1}\mathbf{A}_{,\vartheta}\ \sin\vartheta - \mathbf{A}_{,r}\ \cos\vartheta\right). \tag{16}$$

The equations of quasi-static equilibrium of the porous medium as a whole are expressed in terms of the total stress $\boldsymbol{\sigma}$ in the format akin to single phase solids,

$$\mathrm{div}\boldsymbol{\sigma} = \mathbf{0}, \tag{17}$$

and the kinematic compatibility conditions between the strain rate $\dot{\boldsymbol{\varepsilon}}$ and the velocity $\mathbf{v}$ of the solid skeleton are as usual

$$\dot{\boldsymbol{\varepsilon}} = (\nabla \mathbf{v})_{\mathrm{Sym}}, \tag{18}$$

where, for any second order tensor $\mathbf{A}$, $(\mathbf{A})_{\mathrm{Sym}} = \left(\mathbf{A} + \mathbf{A}^T\right)/2$.
In addition to (18), the plane strain condition implies

$$\dot{\varepsilon}_{33} = \mathrm{v}_3 = 0. \tag{19}$$

Constitutive Eqs. (14) and (15) together with quasi-static equilibrium (17) and kinematic compatibility conditions (18), form a system of first order partial differential equations which governs the problem of the crack propagation. The solution to this system is sought in a separated variables form, by considering asymptotic expansions of near crack-tip fields with a single term. To this purpose, we first prove the following

**Proposition.** The pore pressure is less singular than the total stress $\boldsymbol{\sigma}$, namely, if $\boldsymbol{\sigma} = O(r^s)$ as $r \to 0$, that is if the total stress is singular as $r^s$, $s < 0$, then the pore pressure behaves as $p = O(r^{s+1})$.

**Proof**. Assume that $\boldsymbol{\sigma} = O(r^s)$ as $r$ tends to zero. The constitutive relation (15) implies that at least one of the conditions $p = O(r^s)$ or $\zeta = O(r^s)$ must be met. Let us assume the validity of the former condition: it follows that

$$\nabla p = O\left(r^{s-1}\right).$$

Then Darcy's law $(5)_1$ also implies that $\mathbf{q} = O(r^{s-1})$, thus

$$\mathrm{div}\mathbf{q} = O\left(r^{s-2}\right),$$

and finally the mass continuity equation $(7)_2$ yields $\dot{\zeta} = O(r^{s-2})$, but this result is not compatible with the constitutive Eq. (15) since $\dot{p} = O(r^{s-1})$ and $\dot{\boldsymbol{\sigma}} = O(r^{s-1})$. Therefore, only the condition $\xi = O(r^s)$ must be considered. Indeed then, the time derivative rule (16) gives $\dot{\zeta} = O(r^{s-1})$ and thus the mass continuity Eq. $(5)_2$ implies $\mathbf{q} = O(r^s)$ so that Darcy's law $(5)_1$ is satisfied if and only if $p = O(r^{s+1})$.

Therefore, *the pore pressure does not display a singularity at the crack-tip* if $-1/2 \leqslant s \leqslant 0$, rather, it tends to vanish as $r$ approaches zero. Thus we have obtained an extension to elastic–plastic porous media displaying linear isotropic hardening of a result that holds for quasi-static crack propagation in poroelastic materials (Rice and Simons, 1976; Atkinson and Craster, 1991). However, while there, the pore pressure behaves as $r^{1/2}$ and the stress field in the solid skeleton has the square-root singularity, here, the exponent $s$ will be found in the interval ]-1/2,0[. The vanishing of the pore pressure as $r$ tends to zero means that for quasi-static conditions the material is effectively *drained* at the crack-tip.

From the above argumentation, the leading order asymptotic expressions of the velocity, stress, pore pressure, mass flux, rate of fluid mass content and strength fields are assumed to be the product of a power function of $r$ times a nondimensional function of $\vartheta$, namely,

$$\mathbf{v}(r,\vartheta)=\frac{c}{s}\left(\frac{r}{R}\right)^{s}\mathbf{w}(\vartheta),\qquad \boldsymbol{\sigma}(r,\vartheta)=E\left(\frac{r}{R}\right)^{s}\mathbf{T}(\vartheta),\quad p(r,\vartheta)=\frac{c}{\kappa}\frac{r}{}\left(\frac{r}{R}\right)^{s}P(\vartheta),$$
$$\mathbf{q}(r,\vartheta)=\rho_0\ c\ \left(\frac{r}{R}\right)^{s}\mathbf{z}(\vartheta),\quad \dot{\zeta}(r,\vartheta)=\frac{c}{r}\left(\frac{r}{R}\right)^{s}\Xi(\vartheta),\quad k(r,\vartheta)=E\left(\frac{r}{R}\right)^{s}\chi(\vartheta). \tag{20}$$

The exponent $s$ of the stress singularity is to be found and $R$ denotes a characteristic dimension of the plastic zone, which remains undetermined since the asymptotic problem is homogeneous. In view of the field representations (20), the strain rate and the rates of stress and pore pressure can be recast in the following format:

$$\dot{\boldsymbol{\varepsilon}}(r,\vartheta)=\frac{c}{r}\left(\frac{r}{R}\right)^{s}\mathbf{D}(\vartheta),\quad \dot{\boldsymbol{\sigma}}(r,\vartheta)=E\frac{c}{r}\left(\frac{r}{R}\right)^{s}\boldsymbol{\Sigma}(\vartheta),\quad \dot{p}(r,\vartheta)=\frac{c^2}{\kappa}\left(\frac{r}{R}\right)^{s}\Pi(\vartheta). \tag{21}$$

Indeed, a substitution of $(20)_1$ and $(21)_1$ into (18) gives

$$\mathbf{D}=\left(s^{-1}\mathbf{w}'\otimes\mathbf{e}_\vartheta+\mathbf{w}\otimes\mathbf{e}_r\right)_{\mathrm{Sym}}, \tag{22}$$

where the suffix $(\ )'$ denotes differentiation with respect to $\vartheta$. Moreover, the time derivative rule (16) can be used to define the intermediate angular functions $\boldsymbol{\Sigma}$ and $\Pi$ in (21), namely:

$$\boldsymbol{\Sigma}=\mathbf{T}'\ \sin\vartheta-s\ \mathbf{T}\ \cos\vartheta,\quad \Pi=P'\ \sin\vartheta-(1+s)P\ \cos\vartheta. \tag{23}$$

Asymptotically, the effective stress $\boldsymbol{\sigma}^*$ coincides with the total stress $\boldsymbol{\sigma}$ since the pore pressure provides higher order contribution only. Then introduction of the asymptotic fields (20) in the yield condition (8) results in

$$f(\boldsymbol{\sigma}^*,\ k)=E\left(\frac{r}{R}\right)^{s}f(\mathbf{T},\ \chi)+o(r^s), \tag{24}$$

and thus, in a neighborhood of the crack-tip the yield condition (8) may be equivalently written as:

$$f(\mathbf{T},\ \chi)=\sqrt{J_2(\mathbf{T})}+\frac{\mu}{3}\mathrm{tr}\mathbf{T}-\chi=0. \tag{25}$$

The gradient to the yield function and plastic flow direction defined in (10) and (12) are independent of $r$:

$$\mathbf{Q}=\frac{\mathrm{dev}\ \mathbf{T}}{2\sqrt{J_2(\mathbf{T})}}+\frac{\mu}{3}\mathbf{I},\quad \mathbf{P}=\frac{\mathrm{dev}\ \mathbf{T}}{2\sqrt{J_2(\mathbf{T})}}+\frac{\beta}{3}\mathbf{I}. \tag{26}$$

A substitution of the asymptotic fields (20) and (21) into the equilibrium Eq. (17) and into the constitutive relations (14) and (15) using the compatibility conditions $(21)_1$, (22) yields at the lowest order:

$$\begin{aligned} &\mathbf{T}'\cdot\mathbf{e}_\vartheta + s\ \mathbf{T}\cdot\mathbf{e}_r = \mathbf{0},\\ &\left(s^{-1}\mathbf{w}'\otimes\mathbf{e}_\vartheta + \mathbf{w}\otimes\mathbf{e}_r\right)_{\mathrm{Sym}} = (1+\nu)\ \mathbf{\Sigma} - \nu\ (\mathrm{tr}\mathbf{\Sigma})\ \mathbf{I} + h^{-1}\langle\mathbf{Q}\cdot\mathbf{\Sigma}\rangle\mathbf{P},\\ &\Xi = \alpha(1-2\nu)\ \mathrm{tr}\mathbf{\Sigma} + h^{-1}\alpha\ \ \beta\ \langle\mathbf{Q}\cdot\mathbf{\Sigma}\rangle. \end{aligned} \tag{27}$$

Note that Eqs. $(27)_{1,2}$ together with the yield condition (25) and definitions $(23)_1$ and (26) coincide with the corresponding field equations governing the quasi-static crack propagation in the *drained* elastic-plastic material of the solid phase. This problem has been previously solved for associative (Bigoni and Radi, 1993) and non-associative (Radi and Bigoni, 1993) flow rules. Therefore, the stress singularity $s$, the amplitudes of the elastic and plastic sectors, as well as unknown stress and velocity fields are already available.

There remains to be determined the pore pressure function $P(\vartheta)$, the mass flux function $\mathbf{z}(\vartheta)$ and the rate of mass fluid content function $\Xi(\vartheta)$. Introduction of the fields (20) for pore pressure, mass flux and rate of mass fluid content into Darcy's law and mass continuity equation (7) yields at the lowest order:

$$\begin{aligned} &z_r = -(1+s)P,\\ &z_\vartheta = -P',\\ &z_{\vartheta,\vartheta} + (1+s)z_r + \Xi = 0. \end{aligned} \tag{28}$$

Thus a substitution of $(28)_{1,2}$ and $(27)_3$ into $(28)_3$ gives an equation for the pore pressure function $P$,

$$P'' + (1+s)^2 P = \alpha\ (1-2\nu)\ \mathrm{tr}\mathbf{\Sigma} + h^{-1}\alpha\ \ \beta\ \langle\mathbf{Q}\cdot\mathbf{\Sigma}\rangle, \tag{29}$$

where the left-hand side coincides with the function $\Xi$. Consequently, once the stress field $\mathbf{T}(\vartheta)$ is known from the solution of the drained problem (27), the expressions of the angular functions $\mathbf{\Sigma}(\vartheta)$ and $\mathbf{Q}(\vartheta)$ in $(23)_1$ and (26) may be introduced into the second order ODEs (29), which can be solved for $P(\vartheta)$, from which $\mathbf{z}(\vartheta)$ and follow by (28).

To illustrate the procedure, we consider Mode I crack propagation: the symmetry condition implies the vanishing of the mass flux component $z_\vartheta$ at $\vartheta=0$, and thus by $(28)_2$ the condition $P'(0)=0$. Moreover, we consider both permeable and impermeable crack faces. For permeable crack flanks, the pore pressure vanishes at $\vartheta=\pi$,

$$P(\pi) = 0, \tag{30}$$

whereas, for impermeable crack faces, the mass flux vanishes at $\vartheta=\pi$, that is by $(28)_2$,

$$P'(\pi) = 0. \tag{31}$$

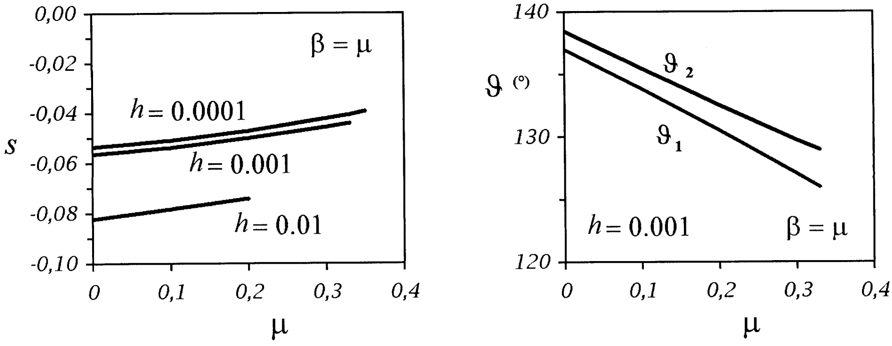


Fig. 1. Variation of (a) stress singularity $s$, (b) elastic unloading and plastic reloading angles with the pressure-sensitivity coefficient $\mu$, for associative flow-rule. A simultaneous increase of the dilatancy and friction coefficients decreases the strength of the singularity $s$.

## 4. Results

As mentioned previously, the singularity $s$, the stress, velocity fields and amplitudes of plastic and elastic sectors at the crack-tip in the drained material are available from Bigoni and Radi (1993) and Radi and Bigoni (1993): in this analysis, these sectors are defined by rays emanating from the crack-tip. For convenience, we report in Fig. 1 the variation with $\mu$ of the stress singularity and the elastic unloading and plastic reloading angles, and in Fig. 2 the stress and velocity angular distributions, in both cases relative to the material parameters $\mu=\beta=0.1$ (associative flow rule). The corresponding plots relative to non-associative flow rule with isochoric plastic flow, namely for $\mu=0.1$, $\beta=0$, are reported in Figs. 3 and 4. All the results refer to the following values of the material parameters: $\alpha=0.5$, $\nu=1/3$ and, except in Fig. 1(a), $h=H/E=0.001$. We recall that these asymptotic solutions defined by (20) are determined except for an amplitude factor, since all the field equations and the assigned boundary conditions are of homogeneous type. As another consequence, the diffusion terms are of higher order in the differential equations. Consequently, the situation is similar to that of a slow crack propagation, and not to that of fast crack propagation: for impermeable crack faces in an elastic porous material, the latter involves a bounded but finite pressure at crack-tip and requires a boundary layer analysis, Rudnicki (1991).

On the basis of the results for the drained solid skeleton, the asymptotic pore pressure field near the crack-tip can be obtained with a numerical integration[1] of (29), using the boundary conditions (30) or (31). In particular, the angular variations of the nondimensional pore pressure $P$ and of the mass flux component $z_\vartheta$ for the case of an associative flow rule $\mu=\beta=0.1$ are reported in Fig. 5. Note that from $(28)_1$ the radial component of the mass flux is proportional to the pore pressure,

[1] The routine DIVPRK of IMSL Library has been used.

with reversed sign, and thus it has not been plotted. The cases of permeable and impermeable crack surfaces are reported in Figs. 5a and b, respectively. For permeable crack faces the pore pressure is positive in a neighborhood of the crack-tip and attains its maximum value ahead of the crack-tip (Fig. 5a). Correspondingly, the pore fluid flux in radial direction is negative and directed towards the crack-tip, which behaves as a sink. For impermeable crack faces, a decrease is found in the pore pressure directly ahead of the crack-tip for $\vartheta < 80°$ (Fig. 5b), which has the effect of weakening the material ahead of the crack-tip and dissipating energy.

The influence of plastic dilatancy on the pore pressure can be read from (29): since $\boldsymbol{\sigma}^*$ is close to the total stress $\boldsymbol{\sigma}$ near the crack-tip, the plasticity condition is asymptotically equivalent to $\mathbf{Q}\cdot\boldsymbol{\Sigma} > 0$; moreover, the plastic contribution on the right hand-side of (29) is predominant for small hardening. Thus, plastic dilatancy corre-

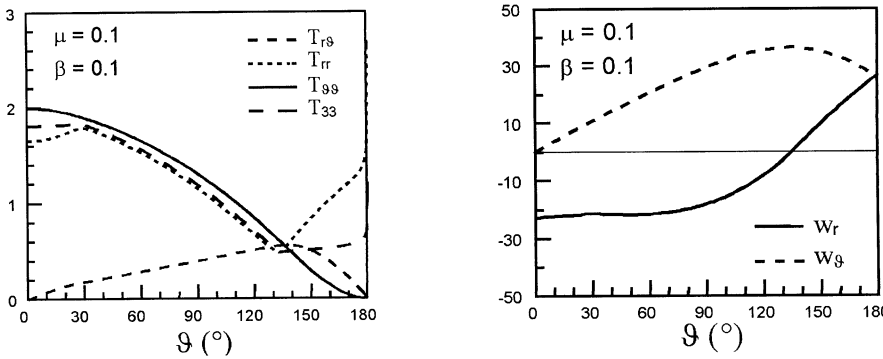


(a) (b)

Fig. 2. (a) Angular variation of stress and (b) velocity angular functions near the crack-tip, for associative flow-rule.

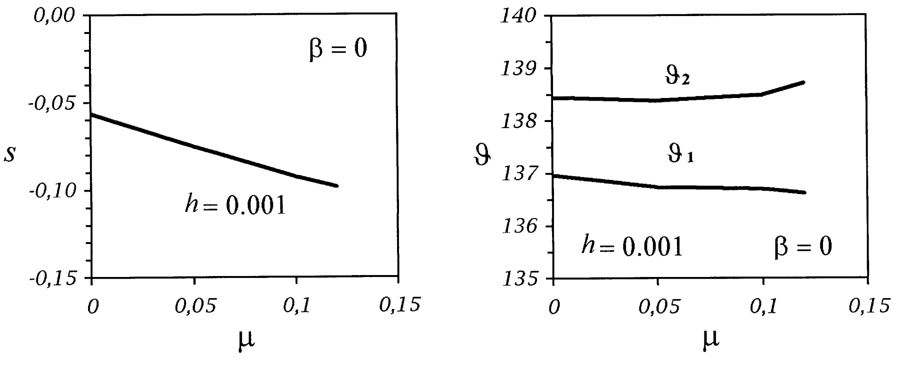


(*a*) (*b*)

Fig. 3. (a) Variation of stress singularity $s$, (b) elastic unloading and plastic reloading angles with the pressure-sensitivity coefficient $\mu$, for non-associative flow-rule. An increase of the non-normality coefficient $\mu$–$\beta$ increases the strength of the singularity $s$.

sponding to $\beta > 0$ increases the pore pressure, and correlatively from $(28)_1$, also the flux towards the crack-tip. Although the occurrence of these two effects seems at first glance paradoxical, it is due to the assumed radial dependence of the fields. On the other hand, the fact that plastic dilatancy triggers the flux towards the crack-tip makes the situation much similar to that of strain-localization where the shear-bands, which are zones of high shearing and dilatancy, attract water, Loret and Prévost (1991). To appreciate the effects of plastic dilatancy on the pore pressure and mass flux fields in the neighborhood of the crack-tip exhibited by Fig. 5a, the situations of small and zero plastic dilatancy are shown in Figs. 6a and b respectively. For small plastic dilatancy, Fig. 6a, the behavior is similar to that of the associative case, Fig. 5a, except for the magnitude of the fields. For a purely isochoric plastic deformation, Fig. 6b, the pore pressure in the diffusing fluid is coupled

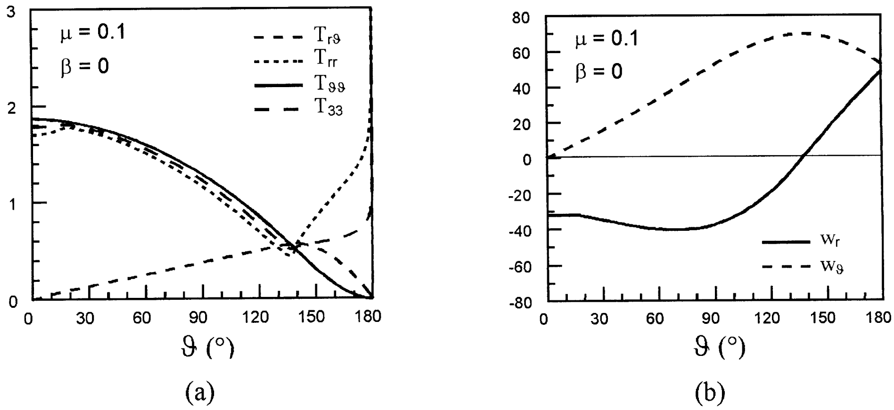


Fig. 4. (a) Angular variation of stress, (b) velocity angular functions near the crack-tip, for non-associative flow-rule.

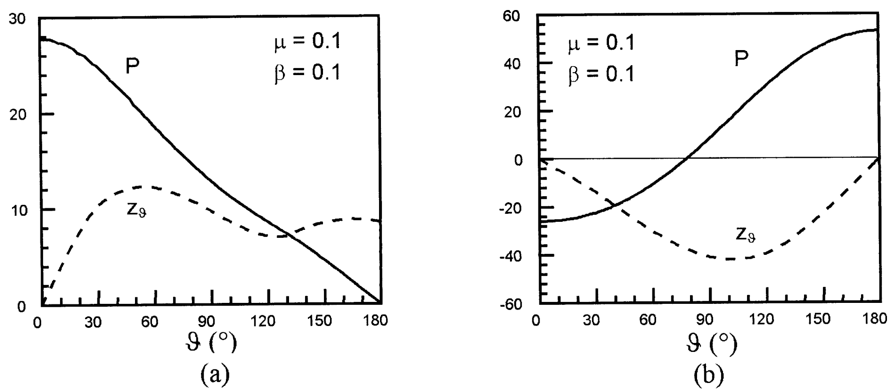


Fig. 5. Angular variation of pore pressure $P$ and mass flux component $z_\vartheta$ near the crack-tip, for (a) permeable and (b) impermeable crack surfaces.

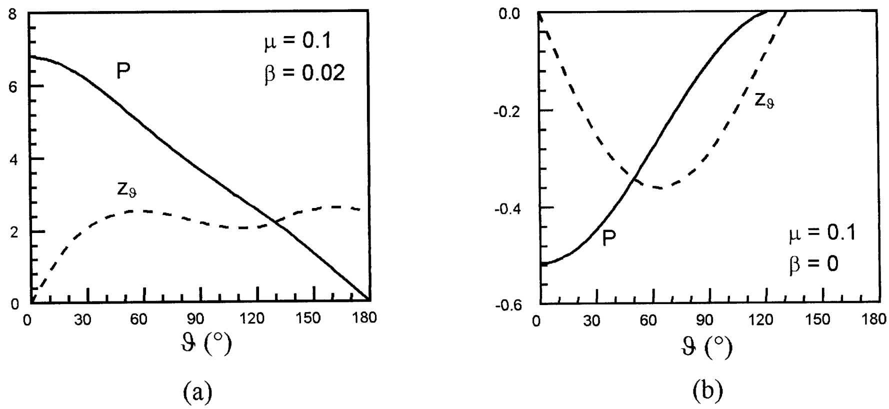


Fig. 6. Angular variation of pore pressure $P$ and mass flux component $z_\vartheta$ near the crack-tip, for (a) small and (b) vanishing plastic dilatancy, relative to permeable crack surfaces. For $\beta=0$, pore pressure is coupled with the elastic volumetric strain, and this changes qualitatively and quantitatively its variations.

with the elastic volumetric dilatation only, and thus it displays a variation similar to the poroelastic case, Atkinson and Craster (1991). This explains why the transition from $\beta>0$ to $\beta=0$ is not smooth. Note also in this case that the fields for permeable crack faces coincide with those for impermeable crack faces, since both pore pressure and mass flux tend to vanish at the crack flanks, namely for $\vartheta>130°$.

The above comments on dilatancy pertain essentially to permeable crack faces. For impermeable crack faces, the pressure is negative ahead of the crack-tip but it increases with $\vartheta$ and is positive along the crack faces (Fig. 5b): therefore, similar to poroelasticity, the flux of water is directed away from the crack in a large fan ahead of the crack.

From the above discussion, it may be concluded that the pore pressure distribution at the crack-tip is strongly influenced by plastic dilatancy. In fact, one can show numerically that increasing the value of the plastic dilatancy $\beta$ or that of the friction coefficient $\mu$ leads to an increase of $s$, that is to a decrease of the stress singularity, see Fig. 1 for the effect of μ. On the other hand, increasing non-associativity, that is the difference $\mu$-$\beta$, leads to an increased stress singularity and has thus destabilizing effects on the crack-propagation, see Fig. 3.

## 5. Conclusions

Steady-state crack propagation has been analyzed in plane strain, Mode I conditions in an elastic-plastic fluid-saturated porous material. The performed analysis is restricted to the leading order terms of the crack-tip fields, neglecting inertial effects. Under this approximation, it is shown that the asymptotic pore pressure and flux fields can be uncoupled from the stress and velocity singular fields. In other words, to solve the problem it is possible, first to determine all asymptotic leading order fields in drained conditions, and second to obtain pore pressure and flux distributions. The underlying reason for that procedure is that, similar to poroelasticity, the pore pressure remains regular at the crack-tip, where it tends to vanish. The obtained numerical results show that the crack-tip pore pressure distribution is very influenced by the plastic dilatancy.

## Acknowledgements

Financial support of M.U.R.S.T. ex 60%–1998 'Propagazione dinamica delta frattura in materiali porosi saturi' (E.R.), M.U.R.S.T. Cofin–1998 'Structural integrity assessment of large dams (D.B.) and GdR Géomécanique des Roches Profondes (B.L.) are gratefully acknowledged.

## References

Achenbach, J.D., Kanninen, M.F., Popelar, C.H., 1981. Crack-tip fields for fast fracture of an elastic-plastic material. J. Mech. Phys. Solids 29, 211–225.
Amazigo, J., Hutchinson, J.W., 1977. Crack-tip fields in steady crack-growth with linear strain hardening. J. Mech. Phys. Solids 25, 81–97.
Atkinson, C., Craster, R.V., 1991. Plane strain fracture in poroelastic media. Proc. Roy. Soc. 434, 605–633.
Bigoni, D., Radi, E., 1993. Mode I crack propagation in elastic-plastic pressure-sensitive materials. Int. J. Solids Structures 30, 899–919.
Bigoni, D., Radi, E., 1996. Asymptotic solution for Mode III crack growth in $J_2$-elasto-plasticity with mixed isotropic-kinematic strain hardening. Int. J. Fracture 77, 77–93.
Biot, M.A., 1941. General theory of three-dimensional consolidation. J. Appl. Phys. 12, 155–164.
Biot, M.A., 1956. The theory of propagation of elastic waves in a fluid saturated porous solid. I. The low frequency range. J. Acoust. Soc. Am. 28, 168–178.
Bose, K., Ponte Castañeda, P., 1992. Stable crack growth under mixed-mode conditions. J. Mech. Phys. Solids 40, 1053–1103.
Cleary, M.P., 1978. Moving singularities in elasto-diffusive solids with applications to fracture propagation. Int. J. Solids Structures 14, 81–97.
Desroches, J., Detournay, E., Lenoach, B., Papanastasiou, P., Pearson, J.R.A., Thiercelin, M., Cheng, A., 1994. The crack tip region in hydraulic fracturing. Proc. R. Soc. Lond. A 447, 39–48.
Herrmann, K.P., Potthast, B., 1995. Asymptotic crack tip fields for pressure-sensitive materials and dynamic crack growth under plane stress conditions. Int. J. Fracture 74, R53–R61.
Johnson, E., Cleary, M.P., 1991. Implications of recent laboratory experimental results for hydraulic fractures. In: Proc. Rocky Mountains Regional Meeting and Low-Permeability Reservoirs Symposium, Denver, pp. 413-428.
Khan, A.S., Xiang, Y., Huang, S., 1991. Behavior of Berea sandstone under confining pressure, Part I: yield and failure surfaces, and nonlinear elastic response. International Journal of Plasticity 7, 607–624.
Khan, A.S., Xiang, Y., Huang, S., 1992. Behavior of Berea sandstone under confining pressure, Part II: elastic-plastic response. International Journal of Plasticity 8, 209–220.
Loret, B., Harireche, O., 1991. Acceleration waves, flutter instability and stationary discontinuities in inelastic porous media. J. Mech. Phys. Solids 39, 569–606.
Loret, B., Prévost, J.H., 1991. Dynamic strain localization in fluid-saturated porous media. J. Engn. Mech., ASCE 117 (4), 907–922.
Östlund, S., Gudmundson, P., 1988. Asymptotic crack-tip fields for dynamic fracture of linear strain-hardening solids. Int. J. Solids Structures 24, 1141–1158.

Papanastasiou, P., 1997. The influence of plasticity in hydraulic fracturing. Int. J. Fracture 84, 61–79.
Papanastasiou, P., Thiercelin, M., 1993. Influence of inelastic rock behaviour in hydraulic fracturing. Int. J. Rock Mech. Min. Sci. & Geomech. Abstr. 30, 1241–1247.
Ponte Castañeda, P., 1987. Asymptotic fields in steady crack growth with linear strain-hardening. J. Mech. Phys. Solids 35, 227–268.
Radi, E., Bigoni, D., 1993. Asymptotic fields of mode I steady-state crack propagation in non-associative elastoplastic solids. Mech. of Materials 14, 239–251.
Radi, E., Bigoni, D., 1994. Crack propagation in porous hardening metals. International Journal of Plasticity 10, 761–793.
Radi, E., Bigoni, D., 1996. Effects of anisotropic hardening on crack propagation in porous ductile materials. J. Mech. Phys. Solids 44, 1475–1508.
Rice, J.R., 1977. Pore pressure effects in inelastic constitutive formations for fissured mass rocks. In: Advances in Civil Engineering through Engineering Mechanics, American Society of Civil Engineers, New York, pp. 360–363.
Rice, J.R., Cleary, M.P., 1976. Some basic stress diffusion solutions for fluid-saturated elastic porous media with compressible constituents. Reviews of Geophysics 14, 227–241.
Rice, J.R., Simons, D.A., 1976. The stabilization of spreading shear faults by coupled deformation-diffusion effects in fluid-infiltrated porous materials. J. Geophys. Res. 81, 5322–5334.
Rudnicki, J.W., 1984. A class of elastic–plastic constitutive laws for brittle rocks. J. Rheology 28, 759–778.
Rudnicki, J.W., 1985. Effect of pore fluid diffusion on deformation and failure of rock. In: Bazant, Z.P. (Ed.), Mechanics of Geomaterials. Wiley, New York, pp. 315–347.
Rudnicki, J.W., 1991. Boundary layer analysis of plane strain shear cracks propagating steadily on an impermeable plane in an elastic diffusive solid. J. Mech. Phys. Solids 39, 201–221.
Rudnicki, J.W., Koutsibelas, D.A., 1991. Steady propagation of plane strain shear cracks on an impermeable plane in an elastic diffusive solid. Int. J. Solids Structures 27, 205–225.
van den Hoek, P., van den Berg, J., Shlyapobersky, J., 1993. Theoretical and experimental investigation of rock dilatancy near the tip of a propagating hydraulic fracture. Int. J. Rock Mech. Min. Sci. & Geomech. Abstr. 30, 1261–1264.
Zhang, R., Zhang, X., Hwang, K. C., 1983. Near-tip crack fields for plane strain, Mode I steady state crack growth in linear hardening material with Bauschinger effect. In: Proc. of ICF Int. Symp. on Fracture Mechanics, Science Press, Beijing, China, pp. 283–290.